ISBN: 978-3-95450-247-9 ISSN: 2673-5490 doi: 10.18429/JACoW-IPAC2024-THPS71

MULTI-PHYSICS AND MULTI-OBJECTIVE DESIGN OPTIMIZATION OF QUADRUPOLE RESONATORS UNDER GEOMETRIC UNCERTAINTIES

P. Putek*[1], G.T. Hallilingaiah[1, 2], S. Adrian[1], University of Rostock, Rostock, Germany
[2]Helmholtz-Zentrum Dresden-Rossendorf, Dresden, Germany
M. Wenskat[3,4], University of Hamburg, Hamburg, Germany
[4]Deutsches Elektronen-Synchrotron DESY, Hamburg, Germany
U. van Rienen[1,5], University of Rostock, Rostock, Germany
[5]Department Life, Light & Matter, Rostock, Germany

Abstract

Exploring the fundamental properties of materials such as niobium, NbTiN, multilayers, or Nb_3Sn in high-precision surface resistance measurements is highly relevant to superconducting radio-frequency (RF) technology. Typically, the calorimetric measurement is carried out with a quadrupole resonator (QPR) to precisely determine the RF properties of superconducting samples. Still, one of the main challenges in the QPR design and operation is to mitigate the impact of microphonics and Lorentz force (LF) detuning, on the one hand, and the RF losses at the adapter flange due the manufacturing tolerances, on the other hand. For this reason, we address the coupled electro-stress-heat problem under geometric uncertainties to study the significant measurement bias of the surface resistance, observed mainly for the third operating mode of the given QPR. We then use a multi-objective and multi-physics shape optimization method to compensate for its influence and find the optimal QPR design in the Pareto sense. Finally, the optimization results and their implications for the QPR operating conditions are discussed to demonstrate the proposed approach.

INTRODUCTION

Superconducting radio frequency (SRF) cavities are widely used in particle accelerators to achieve high acceleration gradients and low losses. Since the power consumption is proportional to the surface resistance R_S, which depends on external parameters such as frequency, temperature, magnetic, and electric fields, precise high-resolution measurements of superconducting material properties are highly demanded. Quadrupole resonators (QPRs) are special dedicated devices used to measure the surface resistance of superconducting samples in a wide parameter space of temperature and RF field strength at three frequencies [1–3,5–9]. These instruments, which cover typical realistic accelerator conditions, consist of a pillbox-like cavity with four vertically arranged hollow rods that bend in the pole shoes at the ends, as shown in Figure 1. This design permits exciting a quadrupole-like magnetic field on the superconducting sample, which yields a measurement of R_S [1] using a calorimetric method. Specifically, the resulting estimated loss on the sample provided by RF simulations of the QPR is measured to evaluate the surface resistance of the sample. The measurement procedure is subject to several uncertainties. In particular, they include the resolution and accuracy of the electronic equipment, which is prone to measurement noise, shape deviations from the cavity design due to the Lorentz force (LF) radiation and atmospheric pressure, flange heating or microphonics, and the Computer-Aided Design (CAD) representation of a physical model reflected by the accuracy of the numerical simulations to name a few of the essential uncertainties. In addition, surface treatment methods such as ultrasonic baths, buffered chemical polishing, and high-pressure rinsing affect the surface roughness [10]. As a result, the accuracy of the surface-resistance measurement performed by a QPR is susceptible to these uncertainties. For these reasons, they must be considered in the modeling phase of the QPR to provide reliable and predictable simulation results. In practice, due to industrial imperfections

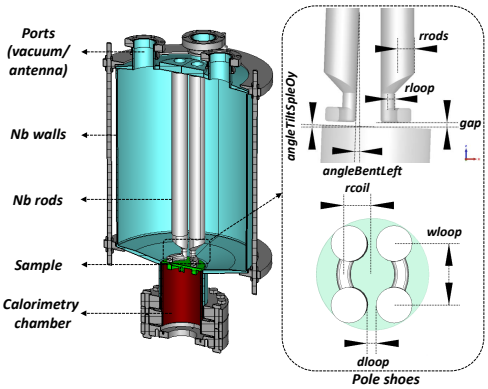

Figure 1: Layout of the QPR (left) with its parameterized model (right) [11].

related to the manufacturing chain in the production process and the harsh operating environment, the operation of the QPR may be affected by a relatively large amount of uncertainty [7]. They may affect the input parameters of physical models, i.e., the material or geometrical parameters at different levels, i.e., model coefficients, force terms, boundary conditions, or physical geometry [12].

The shape of the QPR may deviate from its nominal design not only due to manufacturing imperfections, which may be static but also due to dynamic physical phenomena associated with electromagnetic radiation pressure or microphonics. In fact, besides microphonics and LF detuning [10, 13, 14], the RF losses on the adapter flange [11, 15, 16], may

* piotr.putek@uni-rostock.de

ISBN: 978-3-95450-247-9 ISSN: 2673-5490 doi: 10.18429/JACoW-IPAC2024-THPS71

result in measurement bias, mainly observed for the third operating mode. Unfortunately, the measurement bias of R_S is also detectable for all the frequency modes of the second edition of CERN-QPR [5]. Regardless of whether the deformation is due to static or dynamic phenomena, according to Slater's theorem [17], any deformation of the cavity shape leads to a detuning of the resonance frequency [3], and consequently, of other merit functions. Consequently, the closest neighboring dipole mode can be excited instead of the proper third quadrupole mode [11].

Our studies deal with the multi-objective (MO) shape optimization constrained by the coupled electromagnetic-stress-heat (E-S-H) problem exclusively with a probabilistic description of uncertain geometric parameters. In particular, the influence of the shape deformation on suitably chosen merit functions is considered using the worst-case expectation method [18].

WORST-CASE EXPECTATION APPROACH

We focus on uncertainties associated with geometric parameters $\mathbf{p} \in \Pi \subset \mathbb{R}^Q$, e.g., those depicted in Figure 1 and use a probabilistic framework to describe input variations as in [19]. Next, we replace $\mathbf{p}(\boldsymbol{\xi})$ by random variables defined on a probability space $(\mathcal{A}, \mathcal{F}, \mathbb{P})$. Since the random variables are assumed to be independent with a probability density function (PDF) $\rho_i : \Gamma_i \to [0,1]$, the joint PDF is defined by $\Gamma := \prod_{i=1}^{Q} \Gamma_i \subset \mathbb{R}^P$ assuming it exists.

Next, given a square-integrable function $g(\mathbf{p}) \in L^2(\Gamma)$, the expected value reads as

$$\mathbb{E}[\, g(\mathbf{p})\,] := \int_\Gamma g(\mathbf{p})\, \rho(\mathbf{p})\, \mathrm{d}\mathbf{p}, \tag{1}$$

which induces the inner product of $g(\mathbf{p}), \upsilon(\mathbf{p}) \in L^2(\Gamma)$

$$\big(\, g(\mathbf{p}), \upsilon(\mathbf{p})\,\big)_{L^2_\rho(\Gamma)} := \int_\Gamma g(\mathbf{p}) \cdot \overline{\upsilon(\mathbf{p})}\, \rho(\mathbf{p})\, \mathrm{d}\mathbf{p}, \tag{2}$$

with the complex conjugate denoted by $\overline{\upsilon(\mathbf{p})}$. The associated norm is $\| g(\mathbf{p}) \|_{L^2_\rho(\Gamma)} := \sqrt{\big(\, g(\mathbf{p}), g(\mathbf{p})\,\big)_{L^2_\rho(\Gamma)}}$.

Now, we want to solve eq. (3) in terms of the eigenpair $(\lambda, \mathbf{h})$ comprised of the eigenvalue $\lambda \in \mathbb{R}^+$ and the magnetic field phasor $\mathbf{h} \in \mathbb{C}^d$, the vector-valued mechanical displacement $\mathbf{u} \in \mathbb{R}^d$, and the temperature $T \in \mathbb{R}$ under geometrical uncertainties. The weak form, including expectations of the variational form defined in the physical space, is given as: Find $(\lambda, \mathbf{h}) \in \mathbb{R}^+ \times V_\rho$ and $\mathbf{h} \not\equiv 0, \mathbf{u}, T \in V_\rho$ such that

$$\mathbb{E}\left[\left\langle \mu_r^{-1} \nabla \times \mathbf{h}, \nabla \times \boldsymbol{\varphi} \right\rangle_{D_\mathrm{c}} - \lambda \left\langle \epsilon_r \mathbf{h}, \boldsymbol{\varphi} \right\rangle_{D_\mathrm{c}}\right] = 0, \tag{3a}$$

$$\mathbb{E}\left[\left\langle \nu \left(\nabla \mathbf{u} + \nabla \mathbf{u}^\top\right) + \eta \left(\nabla \cdot \mathbf{u}\right) \boldsymbol{I}, \nabla \boldsymbol{\upsilon} \right\rangle_{D_\mathrm{w}}\right] = 0, \tag{3b}$$

$$\mathbb{E}\left[\left\langle \kappa \nabla T, \nabla \vartheta \right\rangle_{D_\mathrm{w}} - \left\langle \frac{\gamma}{\epsilon \omega} |\nabla \times \mathbf{h}|^2, \vartheta \right\rangle_{D_\mathrm{w}}\right] = 0, \tag{3c}$$

imposed with the LF pressure on the boundary of the rods

$$\mathbb{E}\left[\left\langle \boldsymbol{\sigma}, \mathbf{n}_\mathrm{w} \right\rangle_{\partial D_\mathrm{cw}}\right] = \mathbb{E}\left[\frac{1}{4}\left\langle \frac{1}{\omega} |\nabla \times \mathbf{h}|^2 + \mu |\mathbf{h}|^2, \mathbf{n}_\mathrm{w} \right\rangle_{\partial D_\mathrm{cw}}\right] \tag{3d}$$

for all test functions $\boldsymbol{\varphi}, \boldsymbol{\upsilon}, \vartheta \in V_\rho$ with the Sobolev space of functions with square-integrable weak gradients and vanishing tangential component of $\mathbf{u}$ on the homogeneous Dirichlet boundary denoted by $V = H_0^1(D)$. In eq. (3), $\omega = 2\pi f \in \mathbb{R}^+$, $\mu \in L^\infty(D)$, and $\epsilon \in L^\infty(D)$ denote the angular frequency, where f is the frequency, the magnetic permeability, and the complex electric permittivity, respectively. The thermal conductivity and the electric conductivity are given by $\kappa \in L^\infty(D)$ and $\gamma \in L^\infty(D)$. Moreover, the stress tensor $\boldsymbol{\sigma} = \boldsymbol{C} \cdot \varepsilon(\mathbf{u})$ is composed of 12 non-vanishing functions of the Lamé coefficients $\eta \in L^\infty(D)$ and $\nu \in L^\infty(D)$, where $\varepsilon(\mathbf{u}) = \frac{1}{2}\left(\nabla \mathbf{u} + \nabla \mathbf{u}^\top\right)$ is the linearized Cauchy-Green strain tensor and $\boldsymbol{C}$ denotes the Cauchy stress tensor that is assumed to be independent of the displacement $\mathbf{u}$.

Furthermore, to find the uncertainty propagation through the stochastic coupled E-T-H problem defined in eq. (3), given a function $f(\boldsymbol{x}, \cdot) \in L^2(\Gamma)$ for $\boldsymbol{x} \in D$, the truncated polynomial chaos (PC) expansion is introduced [11, 19, 20]

$$f(\boldsymbol{x}, \mathbf{p}) \doteq \sum_{i=0}^{N} \widetilde{f_{\boldsymbol{i}}}\, \Phi_i(\mathbf{p}), \quad \widetilde{f_{\boldsymbol{i}}} \in \mathbb{C}, \tag{4}$$

with *a priori unknown* coefficient functions to be determined using multidimensional quadrature [21]

$$\widetilde{f_i} \doteq \sum_{k=1}^{K} w_k\, f\left(\mathbf{p}^{(k)}\right)\, \Phi_{\boldsymbol{i}}\left(\mathbf{p}^{(k)}\right), \quad i \in \mathbb{N}_0, \tag{5}$$

where $\Phi_i(\mathbf{p})$ denotes the multivariate PC basis corresponding to the PDF used to model the input variations. Once the polynomial coefficients are found by eq. (5), the expectation value and variance can be estimated using

$$\mathbb{E}\left[f\left(\mathbf{p}\right)\right] = \tilde{f}_0, \quad \mathrm{Var}\left[f\left(\mathbf{p}\right)\right] = \sum_{i=1}^{N} \left|\, \tilde{f}_i \,\right|^2. \tag{6}$$

Next, to find the influence of the deformation due to the LF radiation pressure on the merit functions in the mean-worst-scenario sense [18, 22], we use the first-order Taylor expansion around the nominal parametric shape $\Omega\left(\mathbf{p}_0\right)$

$$\Delta F_j\left[\Omega(\overline{\mathbf{p}})\right] = \sup_{\Omega(\mathbf{p}) \in \Pi} \mathbb{E}\left[f_j\left(\Omega\left(\mathbf{p}\right)\right) - f_j\left(\Omega\left(\mathbf{p}_0\right)\right)\right], \tag{7}$$

and estimate the change of the functions f_j, $j = 1, \ldots, J$. Here, the shape derivative $\mathrm{d}\, f_j$ of the functional $f_j\left(\Omega\right)$ evaluated at $\Omega^{(k)} := \Omega\left(\mathbf{p}^{(k)}\right)$ is introduced in a weak sense [23]

$$\left\langle \mathrm{d}\psi\left(\Omega^{(k)}\right), \mathbf{v} \cdot \boldsymbol{n} \right\rangle = \lim_{\tau \to 0^+} \frac{\psi\left[T_\tau^{\mathbf{v}}\left(\Omega^{(k)}\right)\right] - \psi\left(\Omega^{(k)}\right)}{\tau}, \tag{8}$$

for all $\mathbf{v} \in W$, where $T_\tau^{\mathbf{v}}\left(\Omega\right)$ represents the transformed domain that is obtained by perturbing the original domain Ω by a certain distance τ in the direction of the vector field $\mathbf{v}$ and $\boldsymbol{n}$ is the unit outward normal to Ω.

ISBN: 978-3-95450-247-9 ISSN: 2673-5490 doi: 10.18429/JACoW-IPAC2024-THPS71

Table 1: Results for the MO Optimization – Parameter Domain

Name	$\Omega^*_{\text{HZB}}(\overline{\mathbf{p}})$ [3]	$\Omega^*_{\text{Sol.A}}(\overline{\mathbf{p}})$ [11]	$\Omega^*_{\text{Sol.C}}(\overline{\mathbf{p}})$
p_1 (gap) [mm]	0.50	0.58	0.51
p_2 (rrods) [mm]	13.00	9.76	9.98
p_3 (hloop) [mm]	10.00	9.72	9.96
p_4 (rloop) [mm]	5.00	5.92	5.01
p_5 (wloop) [mm]	44.00	43.79	43.64
p_6 (dloop) [mm]	6.00	4.00	4.11
p_7 (rcoil) [mm]	22.408	25.00	23.57
p_8 (rsample) [mm]	37.50	35.00	35.01
p_9 (ltrans1) [mm]	7.50	7.50	7.26
p_{10} (drrods) [mm]	2.00	2.00	2.25
p_{11} (ltrans2) [mm]	15.00	15.00	15.00

Table 2: Results of the MO Optimization for the Third Mode – Objective Space

Means/Configurations	$\Omega^*_{\text{HZB}}(\overline{\mathbf{p}})$	$\Omega^*_{\text{Sol.A}}(\overline{\mathbf{p}})$	[%]	$\Omega^*_{\text{Sol.C}}(\overline{\mathbf{p}})$	[%]
$F_1(\Omega^*(\overline{\mathbf{p}}), \mathbf{h}, \mathbf{u})$ [M A^2/J]	70.62	88.84	25.80	87.50	23.90
$F_2(\Omega^*(\overline{\mathbf{p}}), \mathbf{h}, \mathbf{u})$ [1/1]	0.11	0.179	62.73	0.152	38.18
$F_3(\Omega^*(\overline{\mathbf{p}}), \mathbf{h}, \mathbf{u})$ [M 1/1]	0.898	2.471	175.17	2.54	182.85
$F_4\Omega^*(\overline{\mathbf{p}}), \mathbf{h}, \mathbf{u})$ [M N/m^2]	0.122	0.111	-9.02	0.113	-7.38

MO MULTI-PHYSICS OPTIMIZATION

Now, in the robust formulation, we use eq. (6) and transform the stochastic merit functions $F_j(\Omega(\mathbf{p}), \cdot)$ as follows

$$F_j\Big(\Omega(\mathbf{p}); \mathbf{h}\Big) := \alpha \mathbb{E}[\, f_j(\,\cdot\,)\,] + (1-\alpha)\sqrt{\text{Var}\left[f_j(\,\cdot\,)\right]}\,, \quad (9)$$

where the prescribed parameter takes the values $0 \leq \alpha \leq 1$. Then, we formulate the robust parametric QPR shape optimization constrained by the E-S-T problem to find the optimal domain $\Omega^*(\mathbf{p})$

$$\inf_{\Omega(\overline{\mathbf{p}}) \in \Xi} \mathcal{J}\Big(\Omega(\mathbf{p}); \mathbf{h}\Big) = \Big[F_1(\,\cdot\,),\ F_2(\,\cdot\,),\ F_3(\,\cdot\,)\Big]^\top, \quad (10a)$$

$$\text{s.t.} \begin{cases} e_1\left(\Omega(\mathbf{p}), [\lambda, \mathbf{h}]\right), & (3a) \\ e_2\left(\Omega(\mathbf{p}), [\mathbf{u}, \mathbf{h}]\right), & (3b) \\ e_3\left(\Omega(\mathbf{p}), [T, \mathbf{h}]\right). & (3c) \end{cases}$$

Finally, to solve eq. (10), we employed the modified steepest descent algorithm with the Lagrange multiplier method and variance-based coefficients as robust gradient [11, 24, 25].

CONCLUSION & DISCUSSION

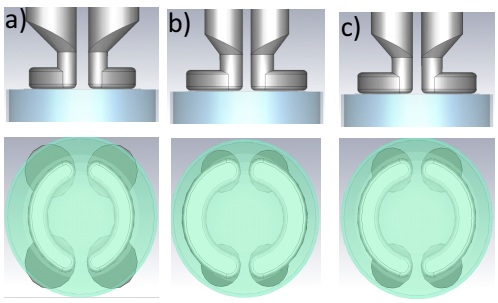

Figure 2: Comparison between the shapes of a) the HZB design [3], b) the design of Sol. A-HZB [11], and c) the obtained solutions Sol. C configuration.

In the proof of concept example, we assumed that the first ten parameters listed in Tab. 1 correspond to the parameterized QPR model, shown in Fig. 1. Thus, we considered $Q = 10$ random design parameters, modeled by a Gaussian distribution such that $\sigma(p_i) = 0.05$ mm. Hermite polynomials of order $d = 2$ were used in the truncated PCE model (4). As objective functionals, we chose the focusing factor $F_1(\cdot)$ to maximize the magnetic field in the area of the sample, the homogeneity factor $F_2(\cdot)$ to improve the resolution of the surface resistance measurements, and finally, the dimensionless factor $F_3(\cdot)$ to mitigate the power loss of conductive materials in the calorimetric chamber caused by the penetrating electromagnetic field as in [11]. We also took into account $F_4(\cdot)$, the maximum LF radiation pressure (the maximum of the displacement magnitude) in the area of the pole shoes, using the Lagrange multipliers method [11]. Next, the Stroud-3 cubature was used [19, 20], which resulted in $K = 20$ deterministic simulations of the QPR model in CST STUDIO SUITE®, as required to estimate the statistical moments given by (6) and (7) applying eq. (8). The resulting design of Sol. C-QPR with a particular focus on the pole shoe domain compared to other QPR configurations is shown in Fig. 2, while the geometric parameters are summarized in Tab. 1. In addition, the values of certain objective functions allow the evaluation of the Sol. C design, are listed in Tab. 2.

We can conclude that the developed UQ-based worst-case expectation analysis of the coupled E-S-T problem permits quantifying the influence of deformations on the QPR's performance. Moreover, using the modified MO steepest descent method to include the peak value of the LF pressure in the pole shoes as a constraint allows for finding the Sol. C-HZB design.

ACKNOWLEDGEMENTS

This work is supported by the BMBF under contract 05H21HRRB1.

ISBN: 978-3-95450-247-9 ISSN: 2673-5490 doi: 10.18429/JACoW-IPAC2024-THPS71

REFERENCES

[1] E. Mahner, S. Calatroni, E. Chiaveri, E. Häbel, and J. M. Tessier, "A new instrument to measure the surface resistance of superconducting samples at 400 MHz," *Rev. of Sci. Instrum.*, vol. 74, no. 7, p. 3390–3394, 2003. doi:10.1063/1.1578157

[2] T. Junginger, "Investigation of the surface resistance of superconducting materials," Ph.D. thesis, University of Heidelberg, 2012.

[3] R. Kleindienst, "Radio Frequency Characterization of Superconductors for Particle Accelerators," PhD dissertation, Universität Siegen, 2017.

[4] R. Kleindienst, O. Kugeler, and J. Knobloch "Development of an Optimized Quadrupole Resonator at HZB," in Proc. 16th Int. Conf. RF Superconductivity SRF2013, Paris, France, 2013, 614–616. doi:10.18429/JACoW-SRF2015-WEA1A04

[5] V. del Pozo Romano, F. Gerigk, R. Betemps, R. I. Fiastre, and T. Mikkola, "Redesign of CERN's Quadrupole Resonator for Testing of Superconducting Samples," in Proc. SRF'17, Lanzhou, China, 2017, pp. 420–422. doi:10.18429/JACoW-SRF2017-TUPB016

[6] S. Bira, M. Ge, A-M. Valente-Feliciano, L. Vega Cid and W. Venturini Delsolaro, "Geometry Optimization for a Quadrupole Resonator at Jefferson Lab," in Proc. 21th Int. Conf. RF Supercond. (SRF'23), Grand Rapids, MI, USA, 2023, pp. 670–673. 10.18429/JACoW-SRF2023-WEPWB048

[7] S. Keckert, "Characterization of Nb_3Sn and multilayer thin films for SRF applications," PhD dissertation, Universität Siegen, 2019.

[8] S. Bira, "Design of a quadrupole resonator for the characterization of the superconducting properties of thin films in radiofrequency regime," PhD dissertation, Universite Paris-Saclay, 2021.

[9] R. Monroy Villa, "Development of a test resonator for investigations of the rf properties of superconducting material," PhD dissertation, Universität Hamburg, 2023.

[10] S. Keckert, T. Junginger, O. Kugeler, J. Knobloch, "The challenge to measure nΩ surface resistance on SRF samples," in Proc. of IPAC'18, Vancouver, Canada, 2018, pp. 2812–2815. doi:10.18429/JACoW-IPAC2018-WEPML049

[11] P. Putek, S. Gorgi Zadeh, M. Wenskat, U. van Rienen, "Multi-objective design optimization of a quadrupole resonator under uncertainties," *Phys. Rev. Accel. Beams*, vol. 25, p. 012002, 2022. doi:10.1103/PhysRevAccelBeams.25.012002

[12] I. Babuška, F. Nobile, and R. Tempone, "A stochastic collocation method for elliptic partial differential equations with random input data," *SIAM J. Numer. Anal.*, vol. 45, no. 3, pp. 1005–1034. doi.org/10.1137/10078635

[13] U. Schreiber, U. van Rienen, "Coupled calculation of electromagnetic fields and mechanical deformation," in Proc. SCEE'06, Sinaia, Romania, 17-22 September 2006, Springer, pp. 63–68, 2006. doi:10.1007/978-3-540-32862-9

[14] J.L. Munoz, F.J. Bermejo, "Lorentz Force Detuning simulations of spoke cavities with different stiffening elements," in Proc. SRF, 2013, pp. 946–949. doi:10.1088/2631-8695/abfdf7

[15] S. Keckert, W. Ackermann, H. De Gersem, X. Jiang, A. Ö. Sezgin, M. Vogel, M. Wenskat, R. Kleindienst, J. Knobloch, O. Kugeler, D. Tikhonov, "Mitigation of parasitic losses in the quadrupole resonator enabling direct measurements of low residual resistances of SRF samples," *AIP Advances*, vol. 11, no. 12, p. 125326, 2021. doi:10.1063/5.0076715

[16] P. Putek, G.T. Hallilingaiah, S.B. Adrian, M. Wenskat, U. van Rienen, "Multi-physics simulation of quadrupole resonators in the time domain under uncertainties," in Proc. 14th IPAC'23, Venice, Italy, 2023, pp. 3063–3066. 10.18429/JACoW-IPAC2023-WEPA182

[17] K. Brackebusch, U. van Rienen, "Investigation of geometric variations for multicell cavities using perturbative methods," *IEEE Trans. Magn.*, vol. 52, no. 3, pp. 1–4, 2015. 10.1109/TMAG.2015.2487542

[18] P. Putek, S. B. Adrian, M. Wenskat, U. van Rienen, "Uncertainty and worst-case expectation analysis for multiphysics QPR simulations," *Supercond. Sci. Technol.* (forthcoming)

[19] D. Xiu, "Efficient Collocational Approach for Parametric Uncertainty Analysis," *Commun. in Comput. Phys.*, vol. 2, no. 2, pp.293–309, 2007.

[20] P. Putek, S. Gorgi Zadeh, M. Wenskat, W Hillert, and U. van Rienen, "Uncertainty quantification of a QuadrupoleResonator for radio frequency characterization of superconductors," in Proc. SRF'19, Dresden, Germany, pp. 1170–1174, 2019. doi:10.18429/JACoW-SRF2019-THP102

[21] D. Xiu, "Numerical Methods for Stochastic Computations: A Spectral Method Approach," *Princeton University Press*, 2010. doi:10.2307/j.ctv7h0skv

[22] A. Shapiro, W. Tekaya, et al. "Worst-case-expectation approach to optimization under uncertainty," *Oper. Res.*, vol. 61, no. 6, pp.1435—1449, 2013.

[23] V. Komkov, "Sensitivity of Functionals with Applications to Engineering Sciences", *Springer-Verlag Berlin Heidelberg New York Tokyo*, 1084. doi:10.1007/BFb0073066

[24] P. Putek, S. Gorgi Zadeh and U. van Rienen, "Multi-Objective Shape Optimization of Tesla-Like Cavities: Addressing Stochastic Maxwell's Eigenproblem Constraints," *J. Comput. Phys.* (forthcoming), Available at SSRN: https://ssrn.com/abstract=4812712, 2024. doi:10.2139/ssrn

[25] B. Sudret, "Global sensitivity analysis using polynomial chaos expansions," *Reliability Engineering & System Safety*, vol. 93, no. 7, pp. 964–979, 2008. doi:10.1016/j.ress.2007.04.002